CHAPTER IV
RESULTS AND DISCUSSION

In this chapter, there are two results to be discussed; the experimental results and numerical results. All of experimental data are shown in Appendix C.1 and all of numerical data are shown in Appendix C.2.

4.1 Experimental

4.1.1 General Condition

The test cell was the model represented from a small section of the Vertical Flux Detector Assembly (VFD) identical to that used in the Point Lepreau Reactor as presented in Chapter 3. The test cell was used to assess the temperature distribution behavior of the moderator by setting the process as similar as that in the nuclear reactor. The set of experiments was showed the heat transfer characteristics of this test cell, which was operated under steady state procedure with electrical heating. The heating element, electrical heater, was designed in the same magnitude level of irradiative heating in the CANDU reactor.

For the previous work, the test cell was operated under the irradiative heating condition by gamma cell. From the result, even if the precision of the measurements was not reliable, however, the steady-state experiment was proved to be the more appropriate manner of the procedure, which it would be used in the nuclear reactor to measure the temperature distribution within the reactor moderator.

To advance of the ultimate conclusion of previous thesis, the improvement of the heating source by using the electrical heater with the same

test cell is described in detail in chapter 3. The electrical heaters could create a large amount of heating similar to the irradiative heating within the station nuclear reactor. This test cell was operated under steady-state condition for collection of data.

For each case, water flow rates, heat generation rates, position of the strap, position of thermocouples and position of the heaters within the test cell were considered the variable parameters of the system.

Thermocouples and heaters were inserted within straws of the test cell, and water allowed to flow through the test cell until temperature equilibrium was achieved after approximately 20 minutes. The electrical source was connected to allow heating by the three electrical heaters. The heat remained constant until thermal equilibrium was achieved after approximately 20 minutes. The data of temperature alteration were collected and shown the data via the connecting computer. The structure of the test cell is shown in Figure 3.1 and the operation process of heat generation by the electrical heater is shown in Figure 3.2.

4.1.2 Irradiative Heating (Gamma Cell)

Some experiments using the gamma cell for irradiative heating of the test cell are shown in detail, Appendix B diagram.

In Figure 4.1, it is the temperature profiles for the irradiative heating by the gamma cell in steady state operation. The water flow rate through the test cell was 0.091 m/s. The position of the thermocouples was 3 cm from the top of the test cell cap. The temperatures of straw 1 and straw 2 increased from 311.4 to 311.8 K and from 310 to 310.5 K, respectively. The temperature differences were only 0.4 and 0.5 K, respectively.

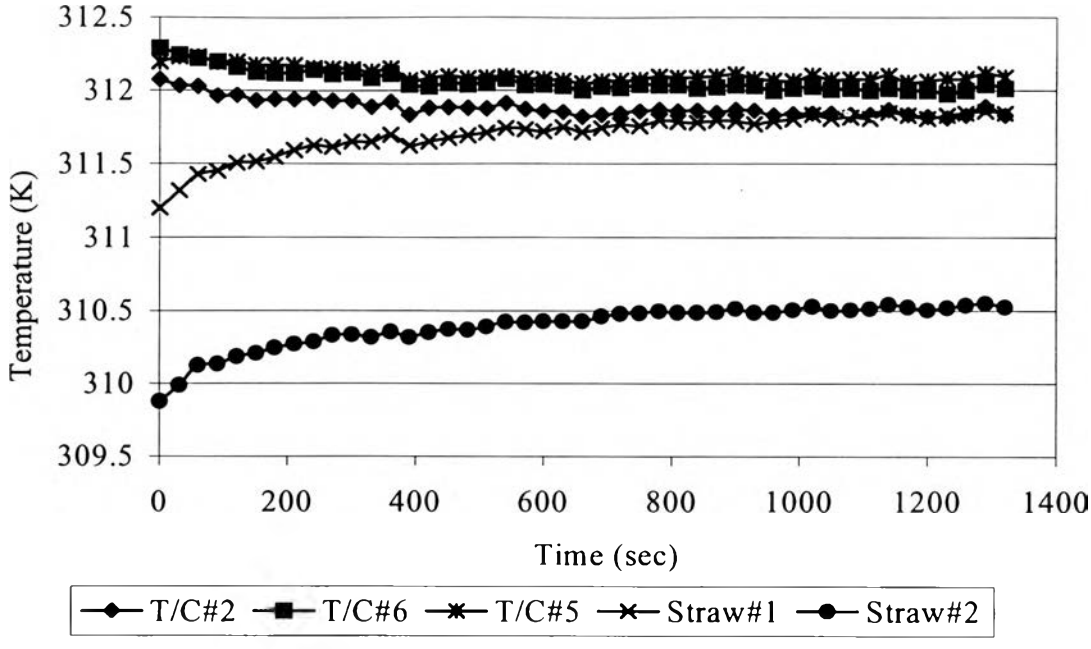

Figure 4.1 Result of gamma heating, 0.091 m/s velocity, thermocouple at 3 cm from top of cap, and strap at the center

Figure 4.2 presents temperature profiles for the irradiative heating by the gamma cell in steady state operation. The water flow rate through the test cell was 0.516 m/s. The position of thermocouples was 3 cm from the top of the test cell cap. The temperatures of straw 1 and straw 2 are increased from 311.9 to 312.6 K and from 311.8 to 312.6 K, respectively. The temperature differences are only 0.7 and 0.8 K, respectively.

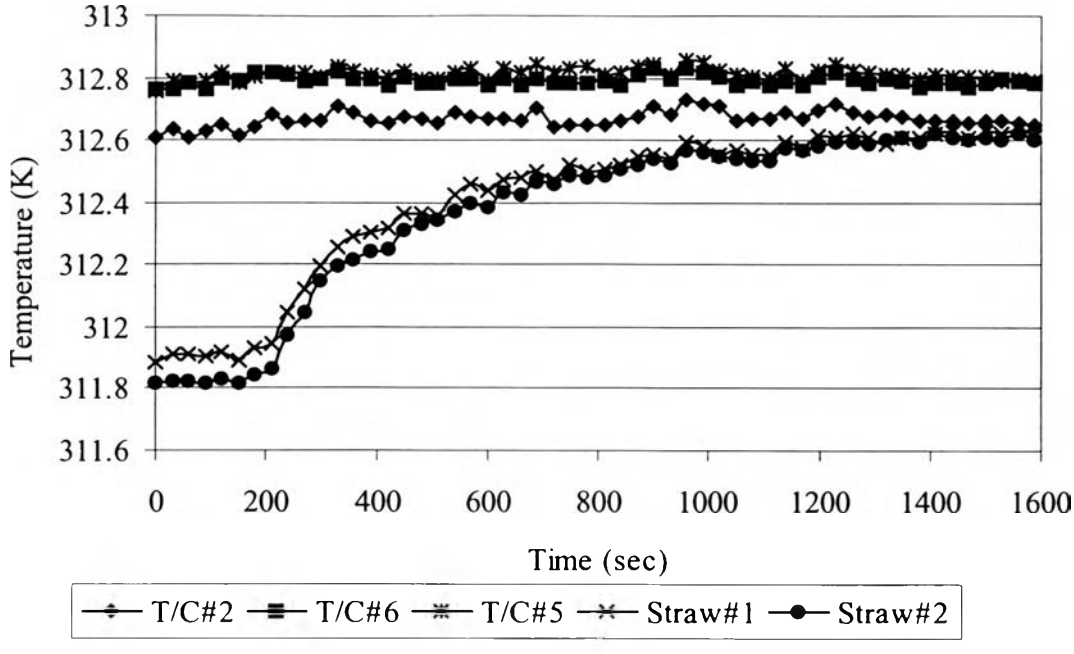

Figure 4.2 Result of gamma heating, 0.516 m/s velocity, thermocouple at 3 cm from top of cap, and strap at the center

Figures 4.1 and 4.2 have the same trends of the temperature profiles. The system took 20 minutes to achieve the first equilibrium and took another 20 minutes to achieve equilibrium after downing the test cell into the gamma cell.

The temperature rise that was determined by the test cell with gamma cell simulating the flux tube assembly in the moderator was less than 1K. This value is too low for precise determination of the heat transfer characteristics of the test cell such as the heat transfer resistances in the various parts of the test cell.

4.1.3 Electrical Heating

The test cell was used with heat generation by electrical heaters. The illustrations of the temperatures at various locations are given in Figure 4.3, for the electrical heating of 4.5 W. The water flow rate through the test cell was 0.27 m/s. The position of thermocouples, the heaters and the strap were at the center of the test cell. The temperatures of straw 1 and straw 2 increased from 298.2 to 342.2 K and from 297.6 to 336.8 K, respectively. The temperature differences were 44 and 39.2 K, respectively.

In Figure 4.4 is the graph of temperature profiles for electrical heating, at 17.5 W. The water flow rate through the test cell was 0.27 m/s. The position of thermocouples, the heaters and the strap were at the center of the test cell. The temperatures of straw 1 and straw 2 increased from 298.1 K to 450.7 K and from 296.8 to 451.5 K, respectively. The temperature differences were 152.6 and 154.7 K, respectively.

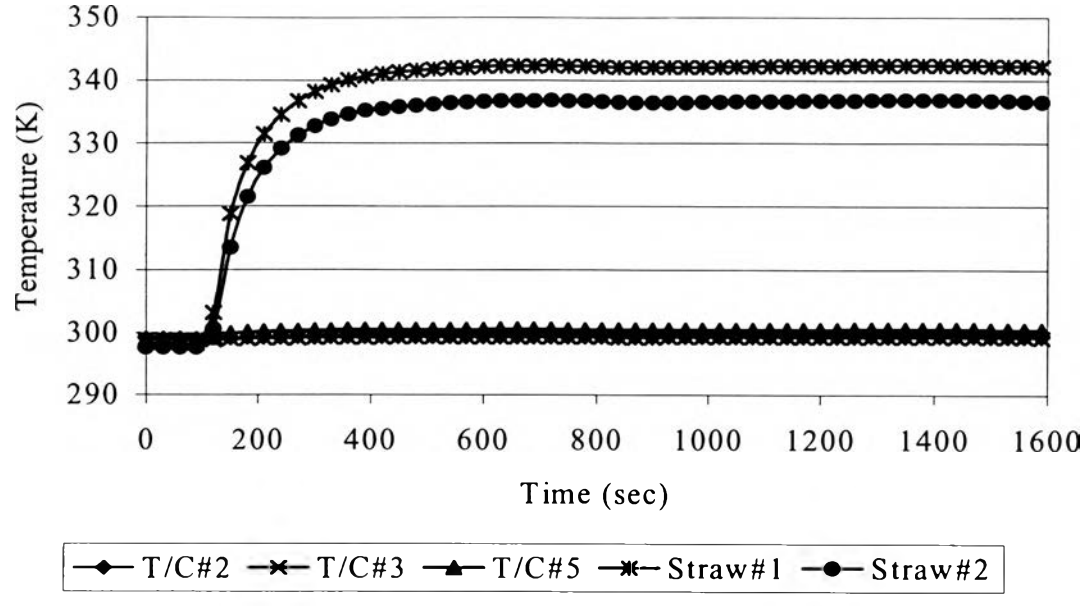

Figure 4.3 Result of electrical heating at 4.5 W, 0.27 m/s velocity and thermocouples, heaters, and strap at the center

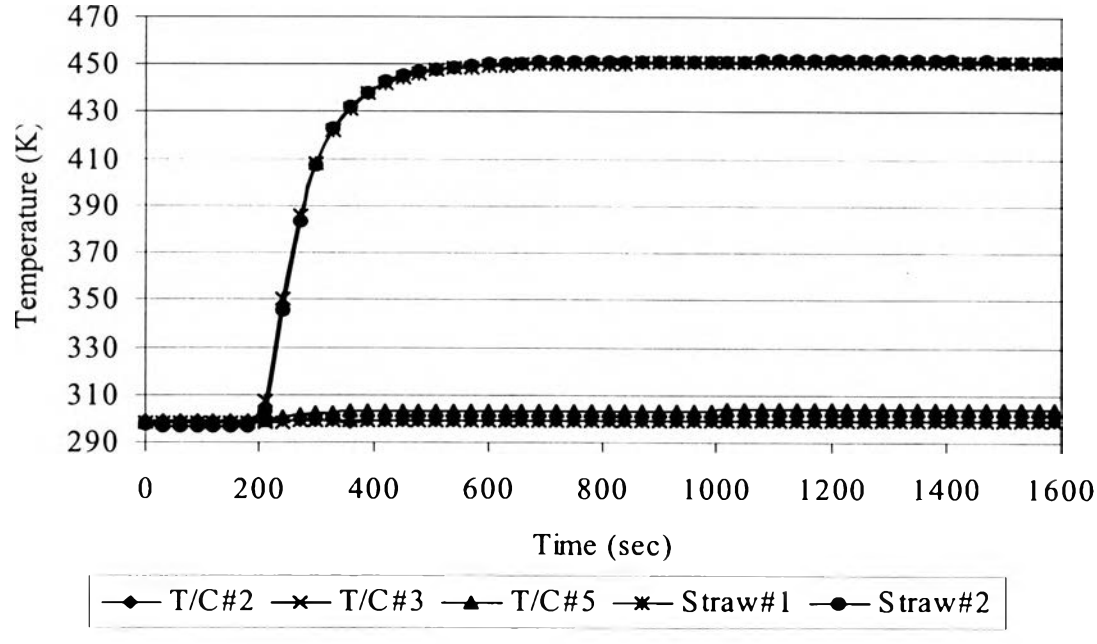

Figure 4.4 Result of electrical heating at 17.5 W, 0.27 m/s velocity and thermocouples, heaters, and strap at the center

In Figure 4.5 is the temperature profiles for the electrical heating, at 4.5 W. The water flow rate through the test cell was 0.96 m/s. The position of the thermocouples, the heaters and the strap were at the center of the test cell. The temperatures of straw 1 and straw 2 increased from 298.7 to 342.0 K and from 297.8 to 337.2 K, respectively. The temperature differences were 43.3 and 39.4 K, respectively.

In Figure 4.6 is the temperature profiles for the electrical heating at 17.5 W. The water flow rate through the test cell was 0.96 m/s. The position of the thermocouples, the heaters and the strap were at the center of the test cell. The temperatures of straw 1 and straw 2 increased from 299.0 to 457.2 K and from 297.5 to 457.6 K, respectively. The temperature differences were 158.2 and 160.1 K, respectively.

From Figures 4.3 to 4.6, it was seem that the characteristics of the temperature profiles are similar when the heating rate and water velocity are changed and gave the same shape as the temperature distribution of the test cell with gamma heating. The electrical heating can be used to simulate the irradiative heating in order to determine the heat transfer characteristic of vertical flux detector assembly.

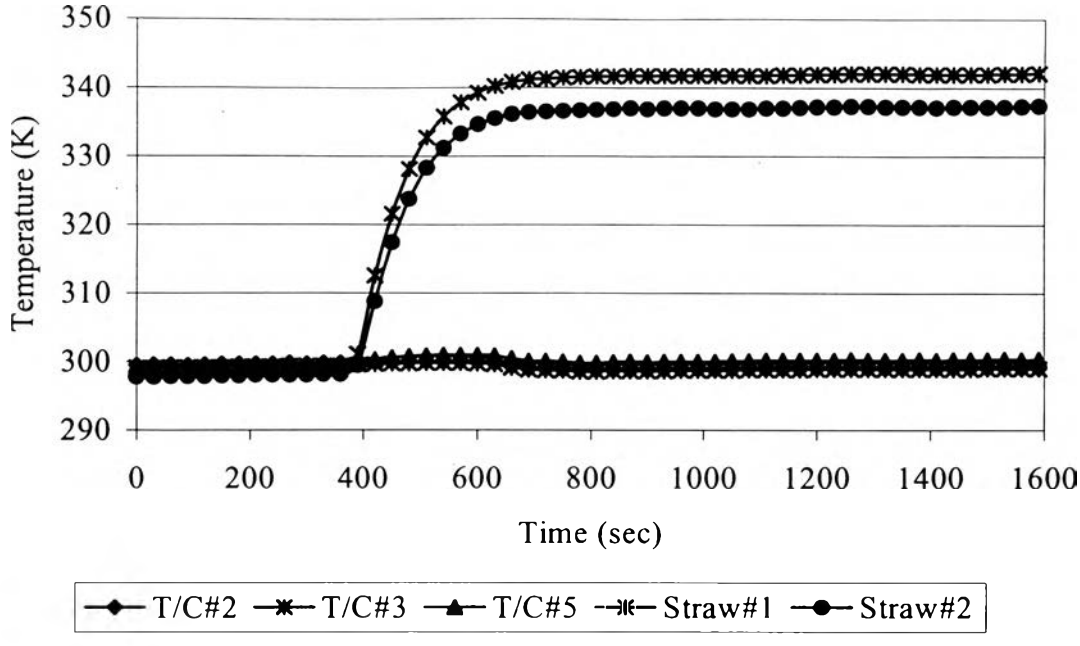

Figure 4.5 Result of electrical heating at 4.5 W, 0.96 m/s velocity and thermocouples, heaters, and strap at the center

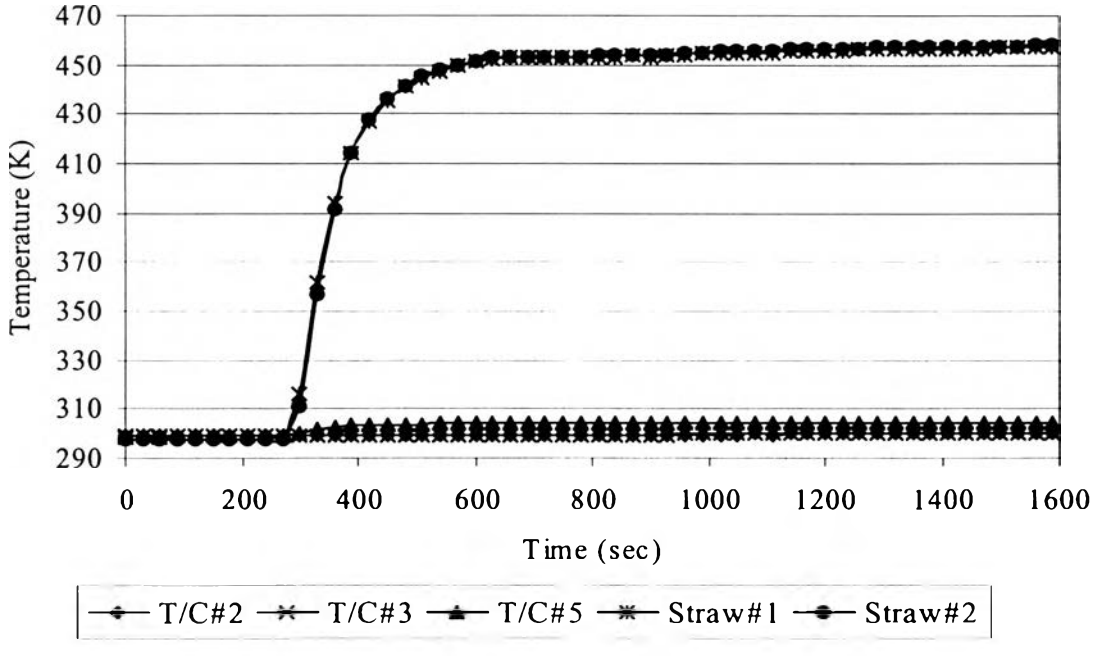

Figure 4.6 Result of electrical heating at 17.5 W, 0.96 m/s velocity and thermocouples, heaters and strap at the center

In case of the various parameters consider the flow rate of the water, which was circulated through the test cell at the constant temperature, approximately 30 °C.

Figures 4.7 and 4.8 show the temperature difference for the variation of water flow rate within the test cell from 0.14 to 0.69 m/s corresponding to heating power equal to 4.5 and 17.5 W, respectively. The values of the temperature differences of thermocouple for the positions of straw 1 and straw 2 that used to measure the temperature inside the bundle of detector wells for various flow rate were similar. For heat generation rate equal to 4.5 W, at the straw1 position, the values are between 42 and 43 K, and the values of straw 2 position are varies from 37 to 39 K for all flow rates. For 17.5 W, the temperature differences of straw 1 position in the test cell are between 149.5 and 151 K, and for straw 2 position, they are between 144.5 and 147.5 K.

The temperature differences of thermocouple 2 and thermocouple 3 are between 0 and 2 K for both heating rates as shown in Figures 4.7 and 4.8. The thermocouple 2 measured the outlet temperature of the test cell and the thermocouple 3 measured the outside surface temperature of the guide tube. Both thermocouples received heat from the electrical heaters generating inside the detector wells.

The temperature rise between the water flowing across the test cell and each straw is not significantly changed due to the various water flow rates of the same generation heat rate. The temperature difference of straw 1 is the highest because of the position closed to the center of bundle and 2 electrical heaters.

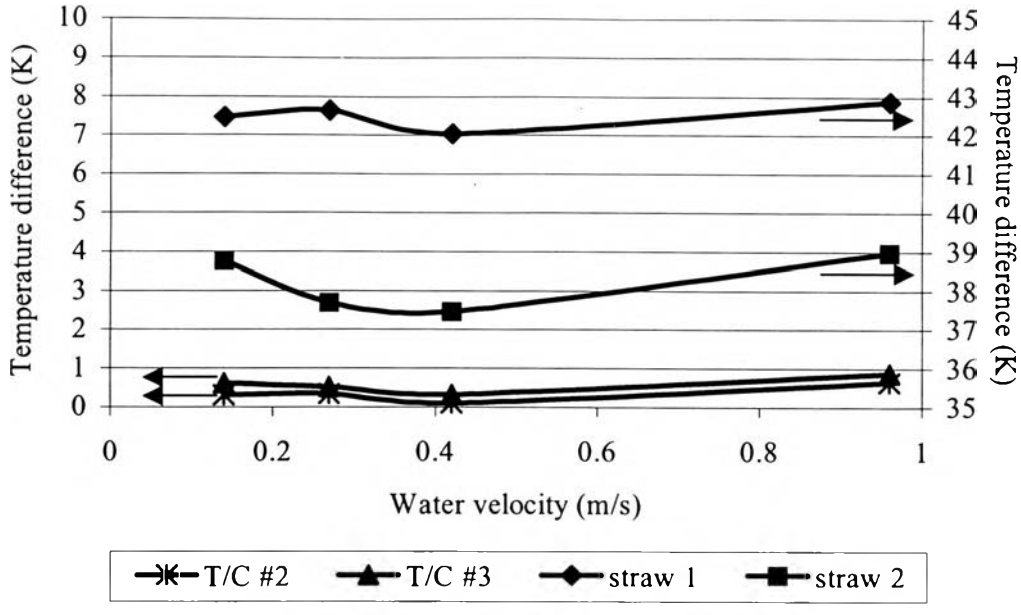

Figure 4.7 Temperature difference of electrical heating at 4.5 W, and heaters, thermocouples and strap at the center

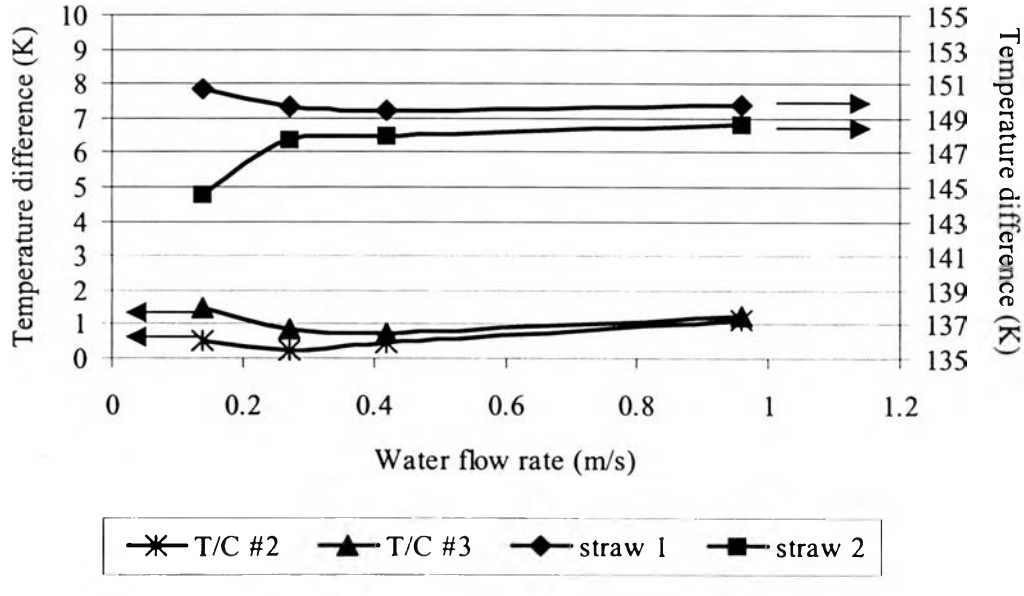

Figure 4.8 Temperature difference of electrical heating at 17.5 W, and heaters, thermocouples and strap at the center

For the case of the position of the electrical heaters as a variable parameter, Table 4.1 shows the temperature difference, when the electrical heater is located at the center of the test cell. Table 4.2 shows the temperature difference, when the electrical heater was located at the bottom of the cap of the test cell. For both cases, the water flow rate is 0.14 m/s, the electrical heating rate is 2.8 W, and the position of the strap is at the center of the test cell. There are the comparisons of the temperature differences for each position of thermocouple number 2 and 3, and thermocouples at straw 1 and straw 2. The temperature difference of each thermocouple for various its position in the two tables is quite close. For Table 4.1, temperature differences are about 0.4, 0.5, 30 and 26.6 K for thermocouple number 2, 3, straw 1 and straw 2, respectively. For Table 4.2, temperature differences are about 0.4, 0.3, 30.3 and 28.8 K for thermocouple number 2, 3, straw 1 and straw 2, respectively. However, these values of straw 1 and straw 2 for the case of the electrical heater at the bottom of the test cell are somewhat higher than ones for the case of the heater at the center of the test cell. Due to the heat loss, for the lower position of the heaters within the test cell, less of heat loss is to the top of test cell. The values for the positions of the thermocouple number 2 and 3 are small, and the distinctions in two tables are less than 1 K.

Table 4.1 Temperature difference of electrical heating at 2.8W, water flow rate at 0.14 m/s, and heaters and strap at the center

Position of T/C from top of the test cell cap (cm)	Distance away from strap (cm)	Temperature difference (K)			
		T/C #2	T/C #3	Straw 1	straw 2
2.5	1	0.4	0.5	24.4	20.4
3.5	0	0.5	0.6	29.9	26.3
4.5	1	0.6	0.5	31.8	27.3
5.5	2	0.3	0.5	28.8	26.1

Table 4.2 Temperature difference of electrical heating at 2.8 W, water flow rate at 0.14 m/s, heaters at bottom and strap at the center

Position of T/C from top of the test cell cap (cm)	Distance away from strap (cm)	Temperature difference (K)			
		T/C #2	T/C #3	straw 1	straw 2
2.5	1	0.2	0.3	16.1	12.4
3.5	0	0.2	0.1	30.0	28.7
4.5	1	0.5	0.3	29.9	28.1
5.5	2	0.9	0.6	31.0	29.6

The results from Figures 4.2 and 4.3 are used for studying the effect of the displacement of the strap. Table 4.2 shows the temperature difference, when the strap was located at the center of the test cell. Table 4.3 shows the temperature difference, which the strap was located at 2.5 cm away

from the center of the test cell. The water flow rate was 0.14 m/s, the electrical heating rate was 2.8 W, and the electrical heaters were at the bottom of the test cell in both cases. For Table 4.3, The temperature differences are about 0.5, 0.4, 28 and 21 K for thermocouple 2, 3, straw 1 and straw 2, respectively. Concerning to the data of temperature difference at the position of straw 1 and straw 2, at the same position of the thermocouple in Table 4.2, the values in Table 4.6 are lower than the ones in Table 4.2. The considered test cell was not long enough to study the effect of the changing of the strap position. However, since the strap was made from metal giving high heat transfer to the capsule tube, the temperature difference near the strap was expected to be less.

Table 4.3 Temperature difference of electrical heating at 2.8W, water flow rate at 0.14 m/s, heater at bottom and strap at 2.5 cm from the top of cap

Position of T/C from top of the test cell cap	Distance away from strap (cm)	Temperature difference (K)			
		T/C #2	T/C #3	straw 1	straw 2
2.5	0	0.3	0.2	15.8	12.2
3.5	1	0.6	0.6	23.3	18.0
4.5	2	0.4	0.5	29.2	21.2
5.5	3	0.5	0.3	32.8	24.2

The internal heat-generation rate by the electrical heaters is the other parameter studied. The electrical heaters in the system were used for simulating the great amount of nuclear reactor heating. Figure 4.9 presents the effect of the heating rate on the temperature difference at the position of straw 1, straw 2 and straw 3 within the test cell. The maximum temperature rise at the heating rate of 17.5W was 170.1 K for straw 1, and 147.9 and 147.4 K for straw 2

and straw 3, respectively. The temperature difference of straw 1 is the highest due to its position close to the center of the bundle of metal tubes and two electrical heaters.

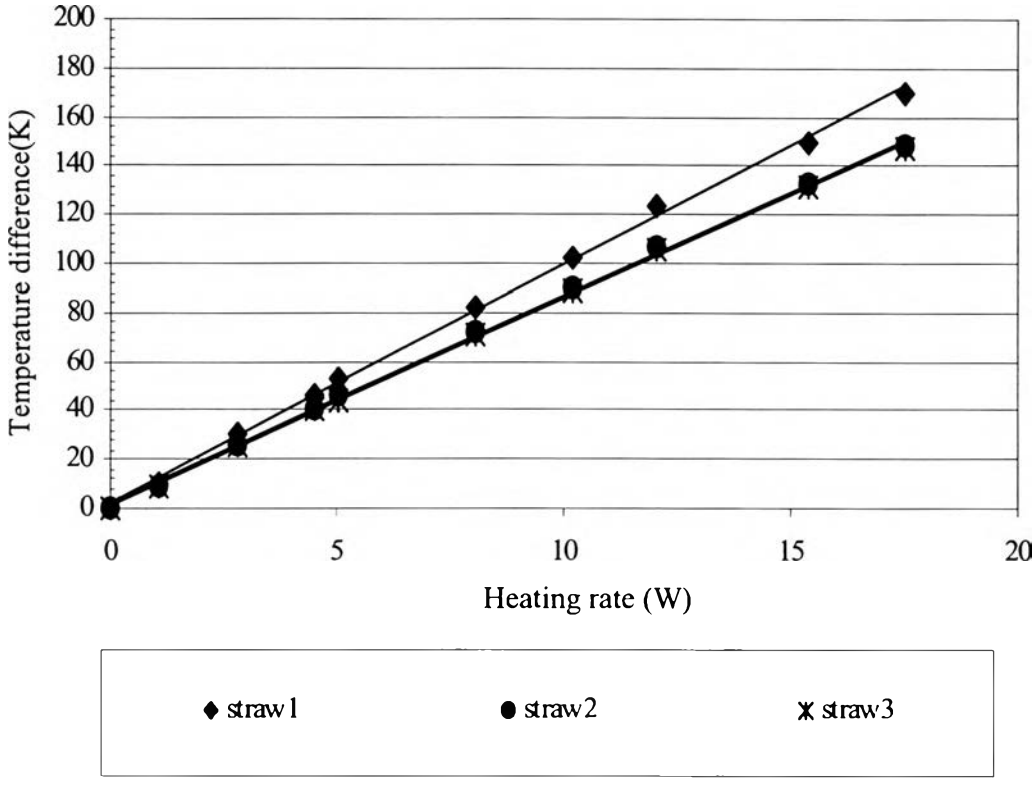

Figure 4.9 Temperature difference vs the rate of heating for various thermocouples

The temperature difference was increased steadily proportionally with the increased rate of heating from the electrical heaters. The slope of the relationship between temperature difference and rate of heating shown in Equation 3.4 was given in the following term:

$$\frac{0.1485}{h_1}+\frac{0.1394}{h_2}+\frac{0.12847}{h_3}+0.1763$$

It is the relationship of heat transfer coefficient between each two layers; center cylinder and inner tube, inner tube and outside tube, and outside tube and the water flowing over the outside tube, and the thermal conductivity.

In order to consider the effect of the position of thermocouples, Figure 4.10 represents the comparison of the temperature difference for any thermocouple position inside the test cell, based on the position of the strap. In this figure, the positions of the strap and electrical heaters were located at the center of the test cell. The comparison is made with two quantities of internal heat-generation rates, 5.04 and 15.38 W. Due to the position of thermocouple within the test cell, the value of temperature rise of straw 1 is more than the one of straw 2 and straw 3, respectively. In three positions, the temperature difference according to power at 15.38 W is larger than the one according to power at 5.04 W. For considering a specified straw, the position of 1 cm below the strap gave the largest temperature difference. This value decreased moderately, while the distance away from the strap is increased to the top of the test cell. The cause of decreased temperature difference when the positions of thermocouples are above the strap position is the heat loss at the top of the test cell to the surrounding air. Unfortunately, the examined teat cell is not long enough to study the value of temperature difference below the position of the strap.

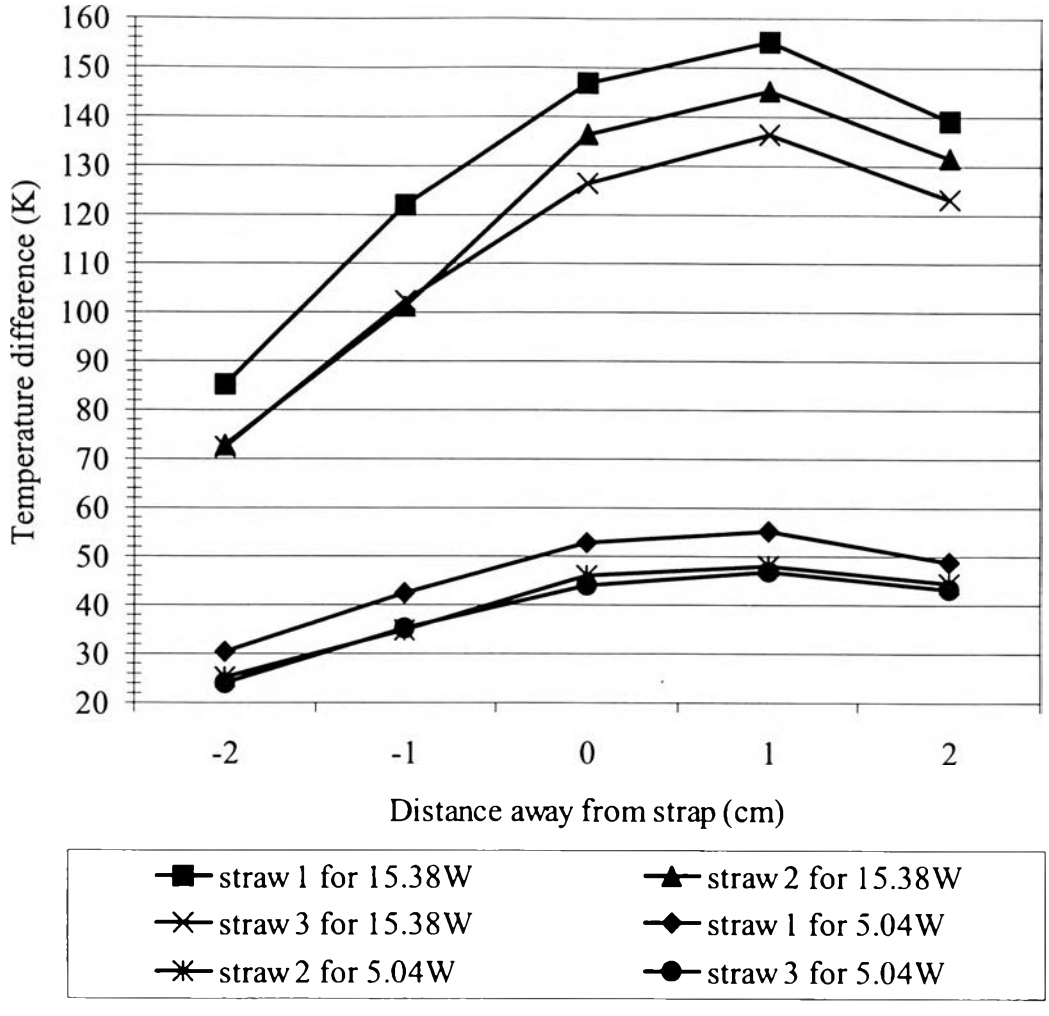

Figure 4.10 Temperature difference of two levels of heat generation for different positions of thermocouples within test cell relative to strap

4.2 Numerical

4.2.1 General Condition

During the present experimental works, studies were made of heat transfer behavior of flux detector assembly used by numerical methods, the computer software named FLUENT.

This program predicted the trends of internal heat flow and temperature rise in the reactor flux detector assembly. In the computer calculation, the model was created for two-dimension steady state heat flux with heat sources of either electrical heating or gamma heating, as presented in Chapter 3. In FLUENT, the criterions of convergence were accomplished for the main properties, an amount of energy, X- and Y- velocity. The criterion of convergence was at least 10^{-6} for energy consideration and at least 10^{-4} for X-, Y-velocity. For this project, each calculation was set at 100 iterations not only meeting the convergence of the computations, but also reaching certain system stability. The model simulated by this program is shown in Figure 3.6.

For the geometry values using in the FLUENT model are:

R_1 = 0.6059 cm (from the center of the test cell)

R_2 = 0.6750 cm (from the center of the test cell)

R_3 = 0.7750 cm (from the center of the test cell)

R_4 = 0.8255 cm (from the center of the test cell)

R_5 = 0.9390 cm (from the center of the test cell)

R_6 = 1.0190 cm (from the center of the test cell)

R_7 = 1.5995 cm (from the center of the test cell)

4.2.2 Numerical Results

In Figures 4.11 and 4.12, the temperature profile of the electrical heating case using air as the fluid 2 with the heat generation rate of 1.11 W/g are presented. The maximum temperature in the model was 514.01 K.

In Figures 4.13 and 4.14, the temperature profile of the gamma heating case using air as the fluid 2 with the heat generation rate of 1.11 W/g are presented. The maximum temperature are in the model was 527.18 K.

In Figures 4.15 and 4.16, the temperature profile of the electrical heating case using helium as the fluid 2 with the heat generation rate of 1.11 W/g are presented. The maximum temperature in the model was 345.11 K.

In Figures 4.17 and 4.18, the temperature profile of the gamma heating case using helium as the fluid 2 with the heat generation rate of 1.11 W/g are presented. The maximum temperature in the model was 360.72 K.

In all of these pictures from Figure 4.11 to Figure 4.18, there are variations of the heat source, the heating rate and material for fluid 2. It is shown that the same trend of the temperature profile occured. The color represents the temperature at any position in the model. The temperature at the bottom layer of the model represents the center cylinder. The temperature here is the highest due to the heat generation with this region. The temperature rise along the model is more pronounced for helium than air. Most of heat passing along the strap but some heat can flow toward the center between the two straps. Due to higher thermal conductivity of helium, this is more pronounce than for air.

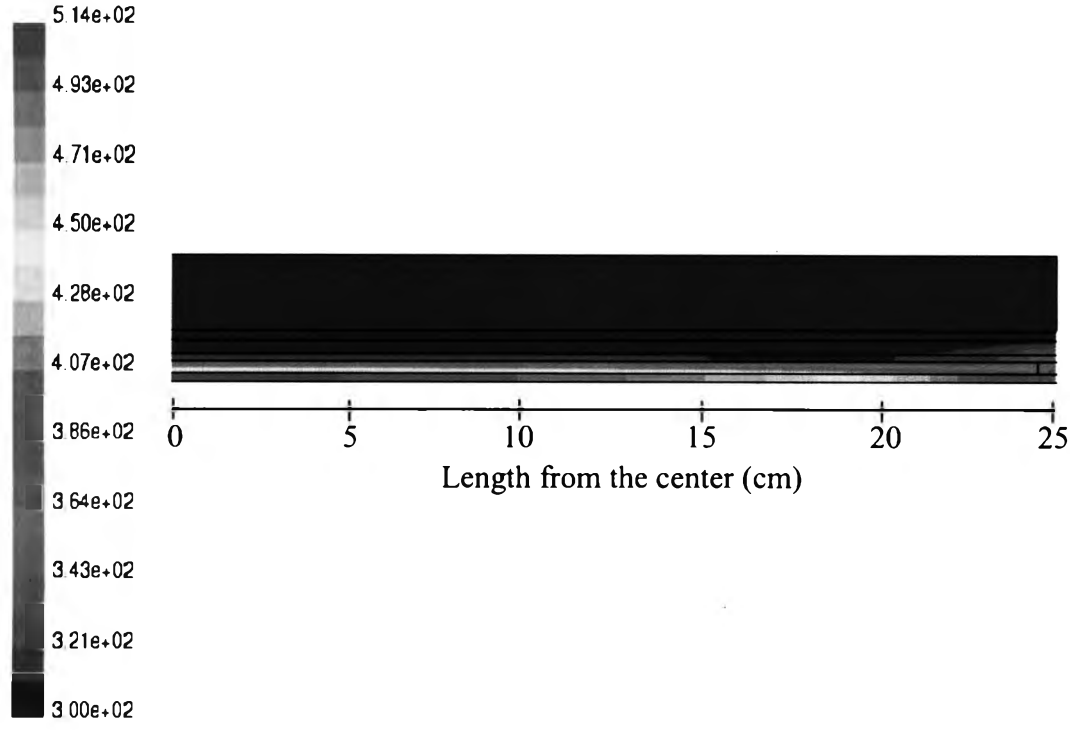

Figure 4.11 Temperature profile for the small part of the test cell with electrical heating at 1.11 W/g and using air

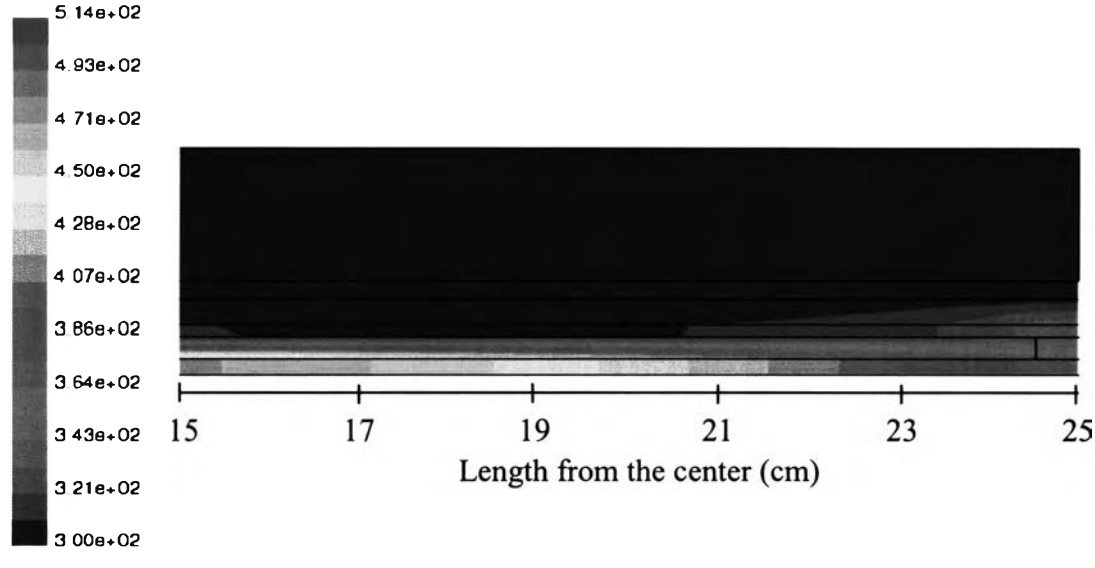

Figure 4.12 Temperature profile for specifying at the strap of the test cell with electrical heating at 1.11 W/g and using air

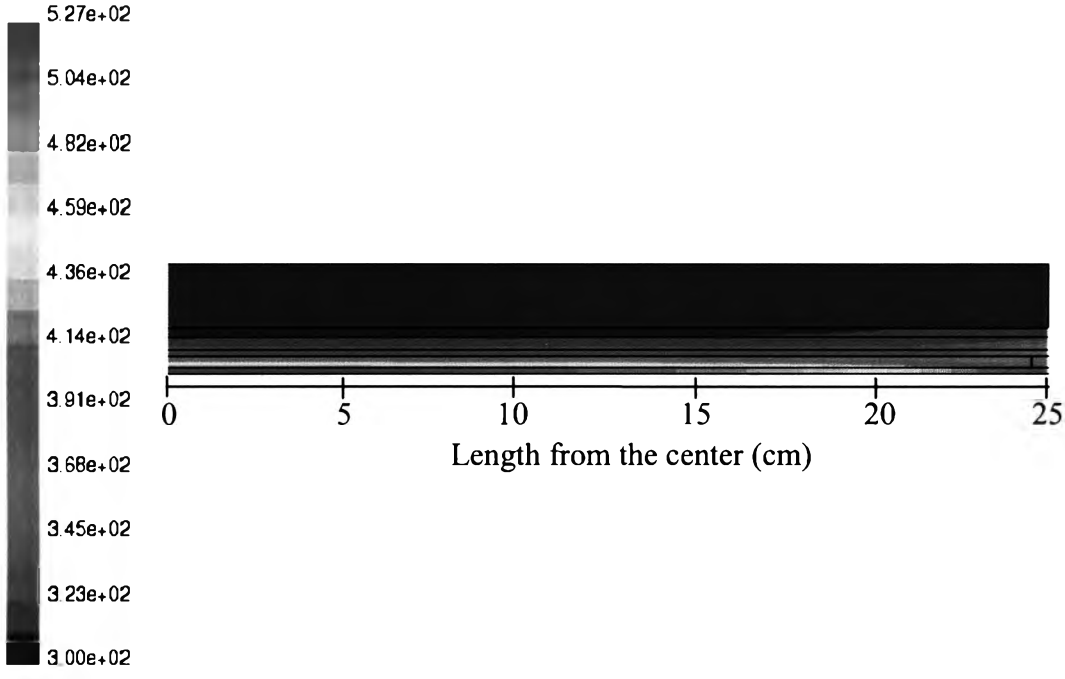

Figure 4.13 Temperature profile for the small part of the test cell with gamma heating at 1.11W/g and using air

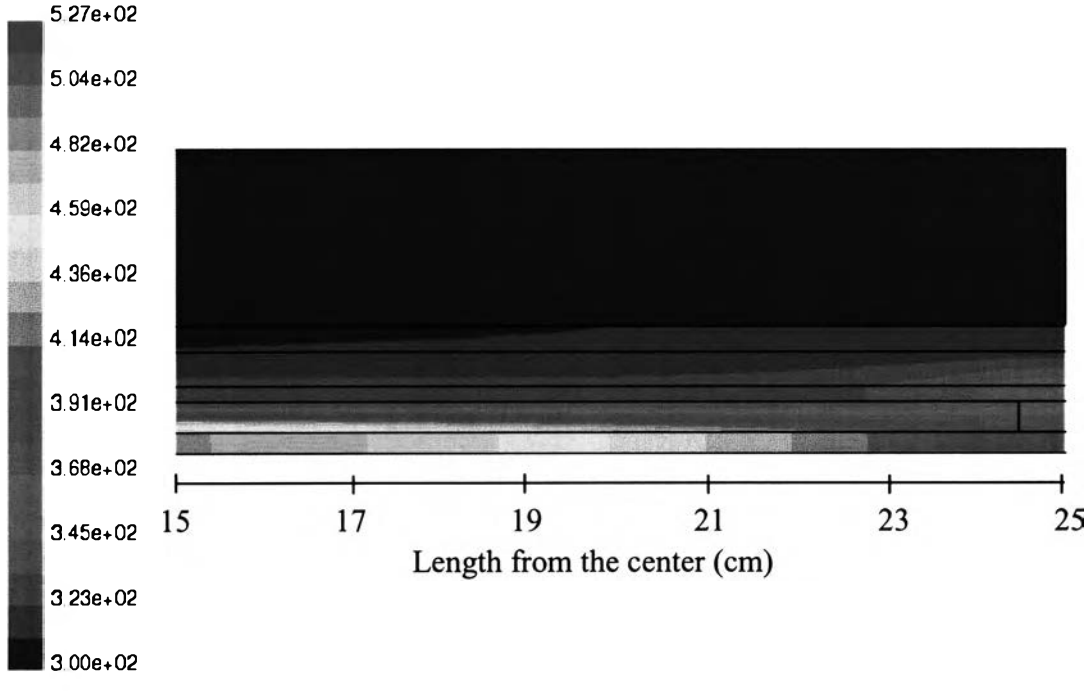

Figure 4.14 Temperature profile specifying at the strap of the test cell with gamma heating at 1.11 W/g cell and using air

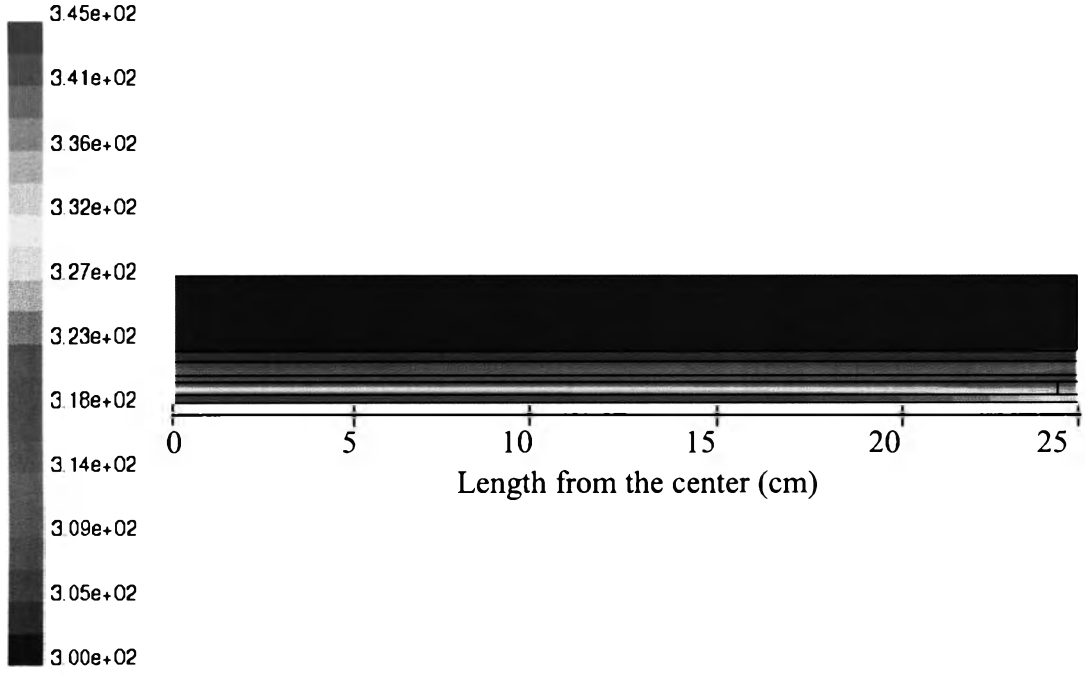

Figure 4.15 Temperature profile for the small part of the test cell with electrical heating at 1.11 W/g and using helium

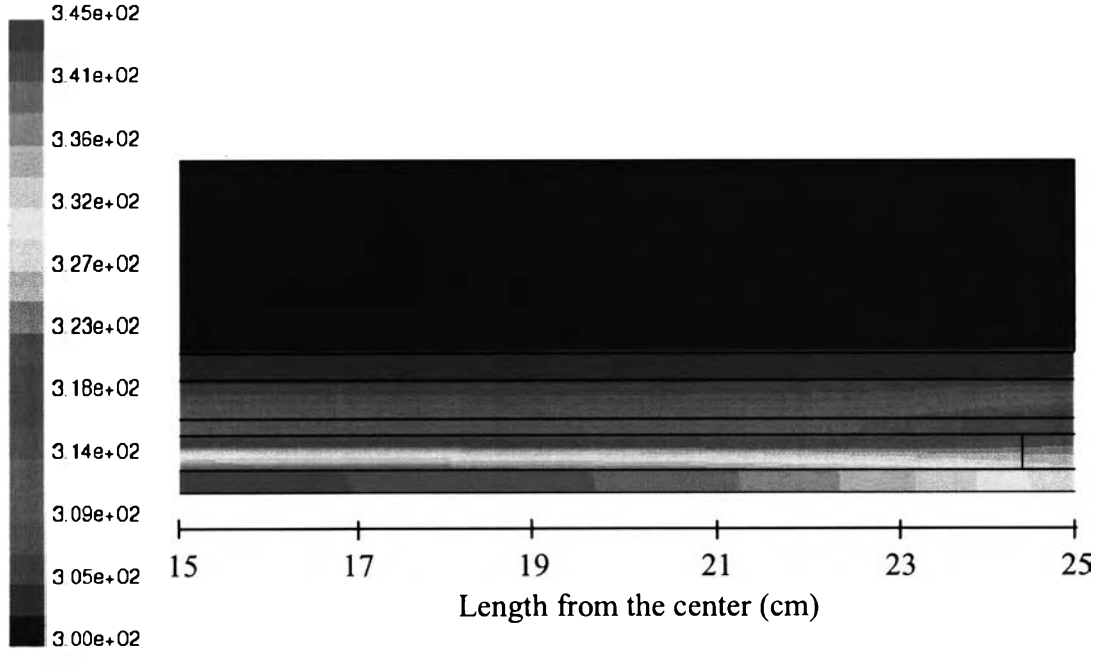

Figure 4.16 Temperature profile for specifying at the strap of the test cell with electrical heating at 1.11 W/g and using helium

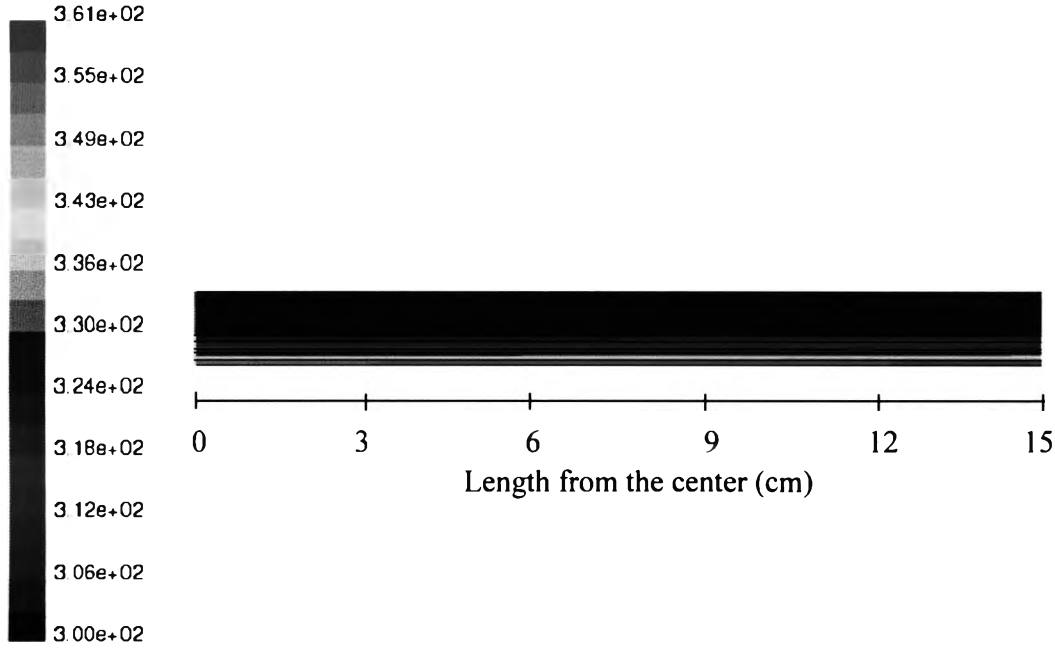

Figure 4.17 Temperature profile for the end part of the test cell with gamma heating at 1.11 W/g and using helium

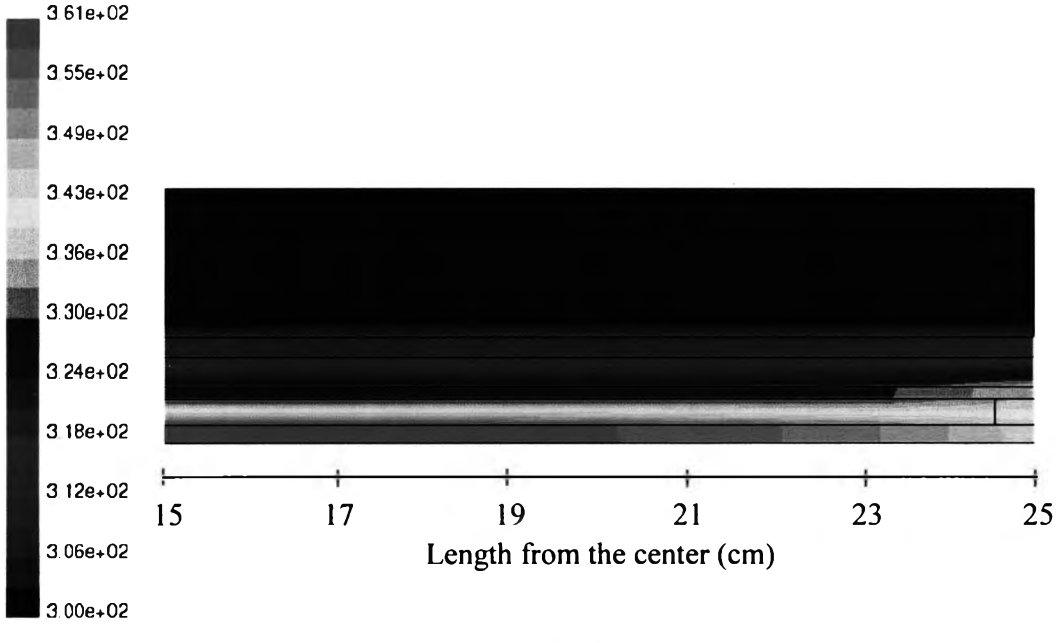

Figure 4.18 Temperature profile for specify at the strap of the test cell with gamma heating at 1.11 W/g and using helium.

In order to examine more detail of the transfer behavior for heating in both cases, electrical heating and gamma heating, the temperatures along the length of the inside surface of the center cylinder (the line R_1) and along the length over the outer tube, the guide tube (the line R_6) are determined.

Figure 4.19 to 4.26 are the temperature profiles from the simulation calculation by FLUENT. Figure 4.19 presents the temperature along the inside surface of the center tube, center cylinder (R_1) for electrical heating using air as fluid 2. The heat generation was 10 W.

Figure 4.20 shows the temperature profiles along the outside surface of the outer tube, guide tube (R_6) for electrical heating using air. The heat generation was 10 W.

Figure 4.21 shows the temperature profiles along the inside surface of the center tube, center cylinder (R_1) for electrical heating using helium as fluid 2. The heat generation was 10 W.

Figure 4.22 shows the temperature profiles along the outside surface of the outer tube, guide tube (R_6) for electrical heating using helium. The heat generation was 10 W.

Figure 4.23 shows the temperature profile along the inside surface of the center tube, center cylinder (R_1) for gamma heating using air as fluid 2. The heat generation was 10 W.

Figure 4.24 shows the temperature profile along the outside surface of the outer tube, guide tube (R_6) for gamma heating using air. The heat generation is 10 W.

Figure 4.25 shows the temperature profile along the inside surface of the center tube, center cylinder (R_1) for gamma heating using helium as fluid 2. The heat generation was 10 W. And, Figure 4.26 shows the temperature profile along the outside surface of the outer tube, guide tube (R_6) for gamma heating using helium. The heat generation was 10 W.

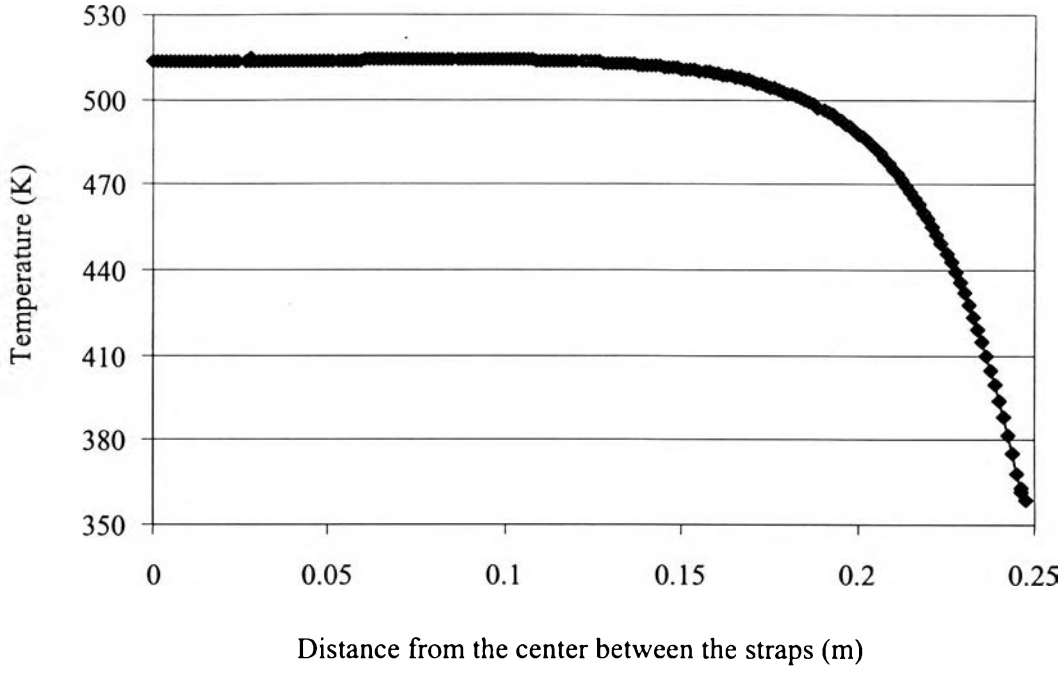

Figure 4.19 The temperature along the inside surface of the center tube, (R_1)for electrical heatingat 10 W with using air

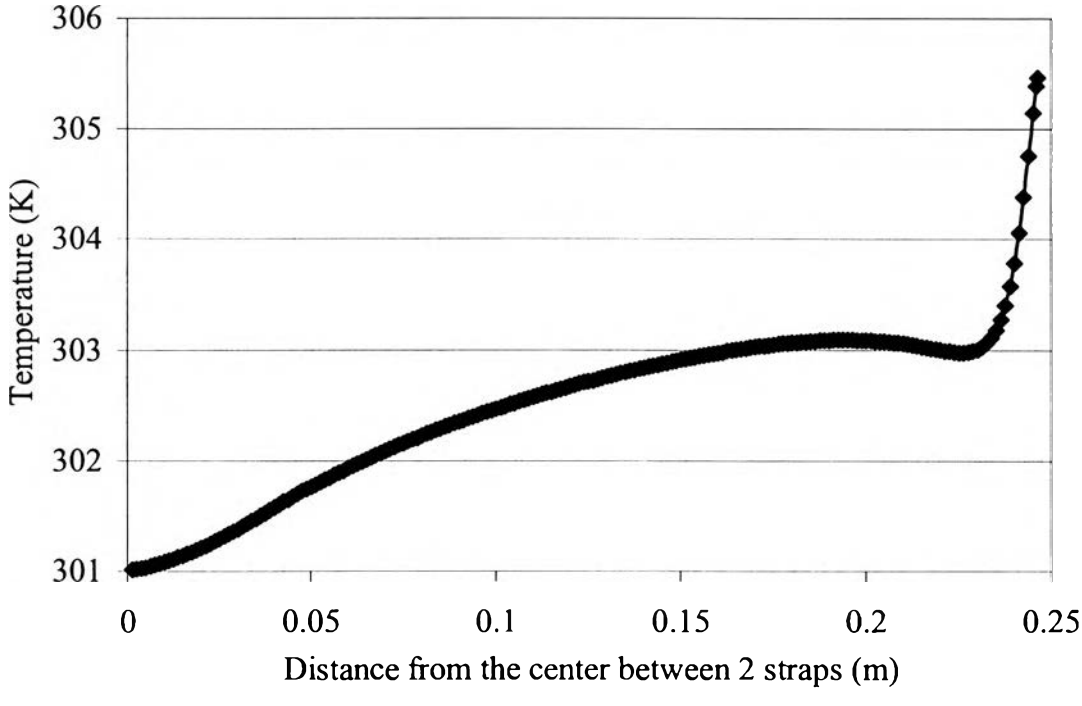

Figure 4.20 The temperature along the outside surface of the outer tube, (R_6) for electrical heating at 10 W with using air

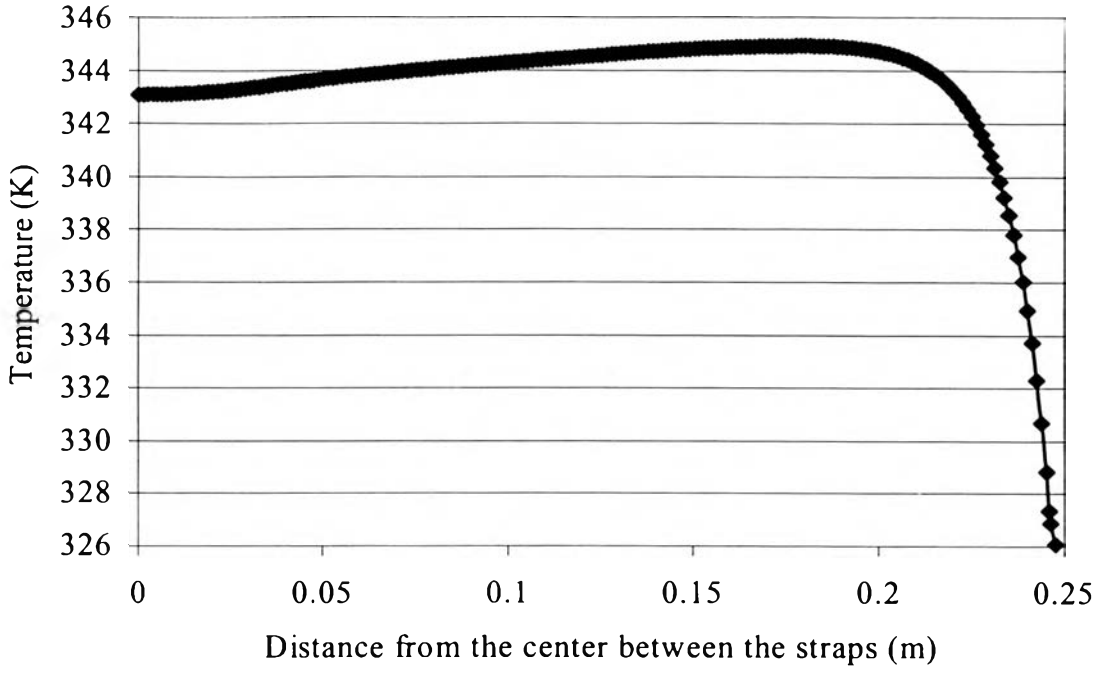

Figure 4.21 The temperature along the inside surface of the center tube, (R_1) for electrical heating at 10 W with using helium

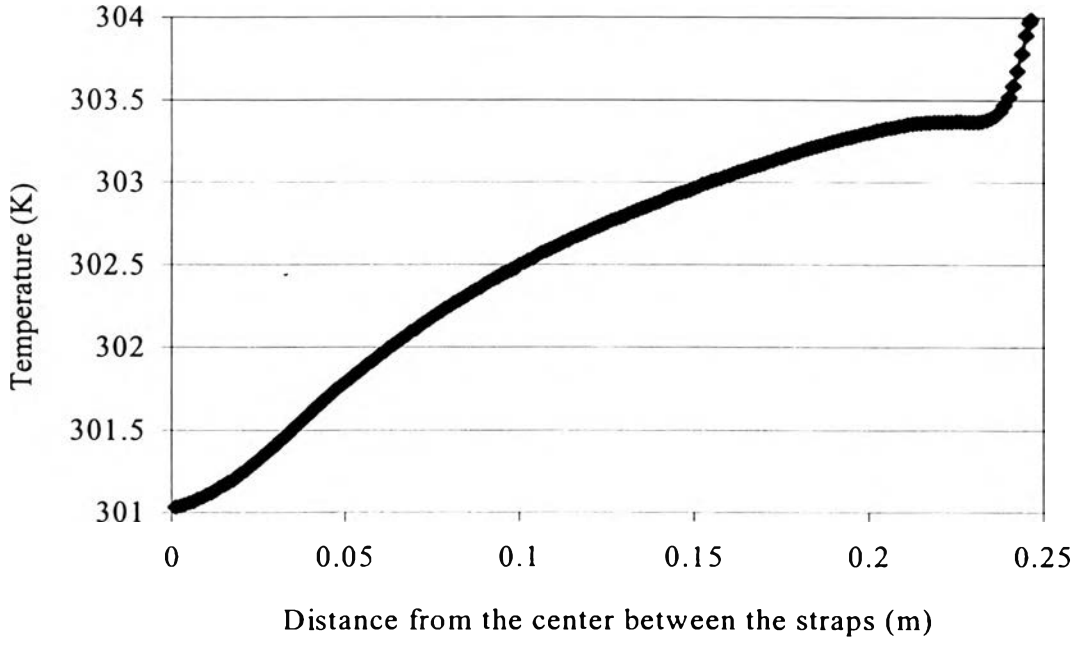

Figure 4.22 The temperature along the outside surface of the outer tube, (R_6) for electrical heating at 10 W with using helium

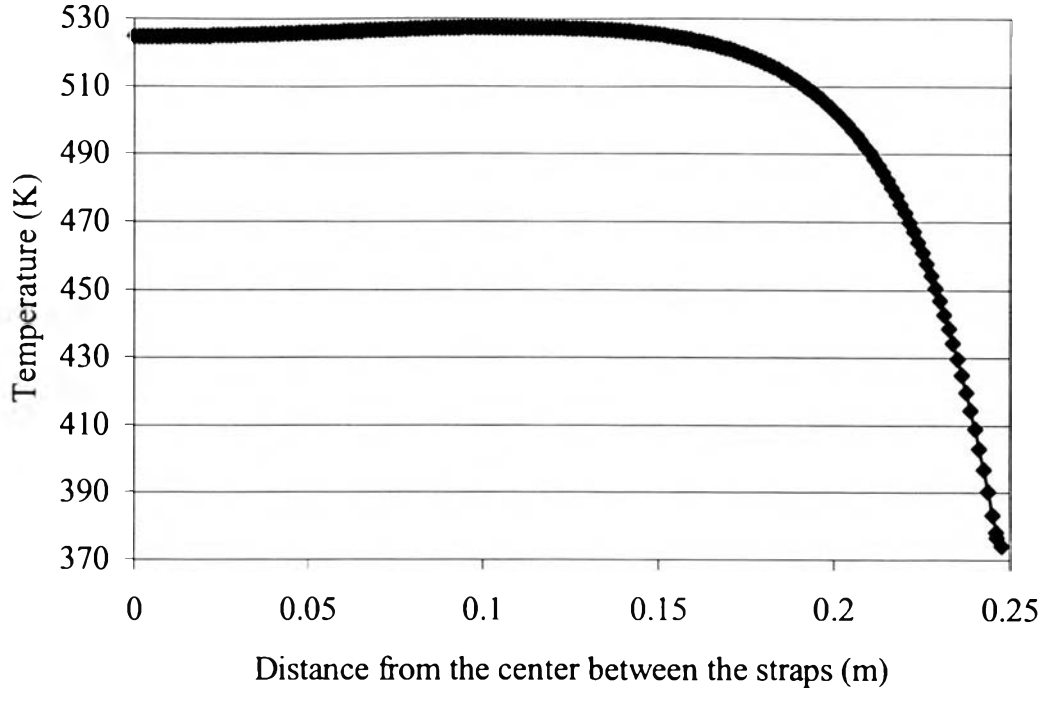

Figure 4.23 The temperature along the inside surface of the center tube, (R_1) for gamma heating at 10 W with using air

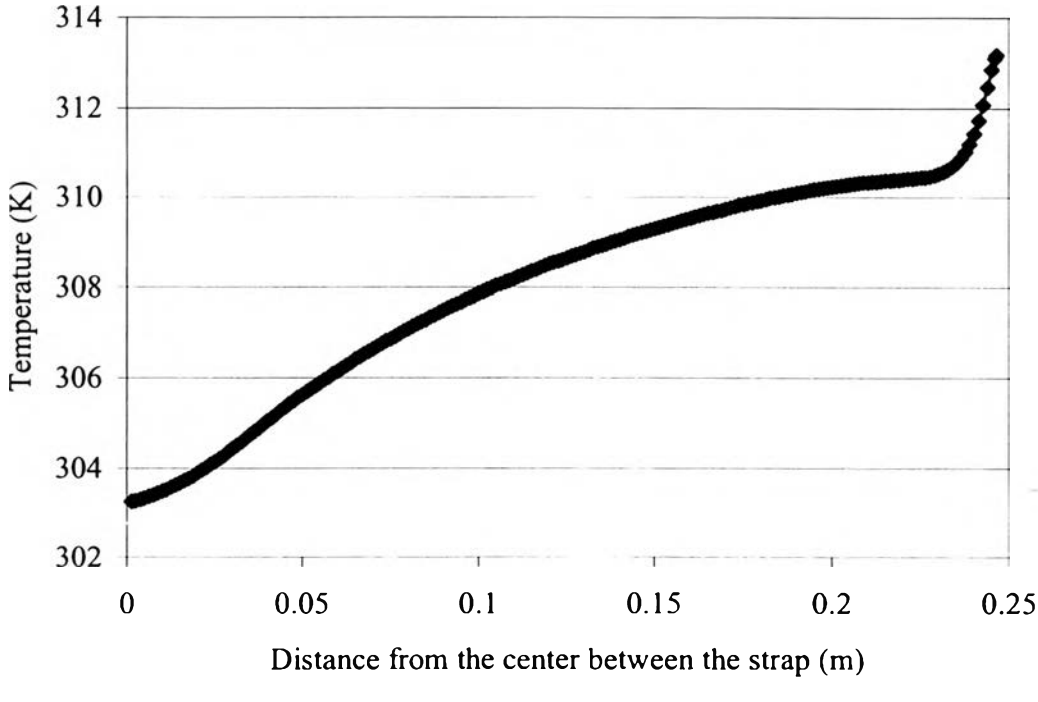

Figure 4.24 The temperature along the outside surface of the outer tube, (R_6) for gamma heating at 10 W with using air

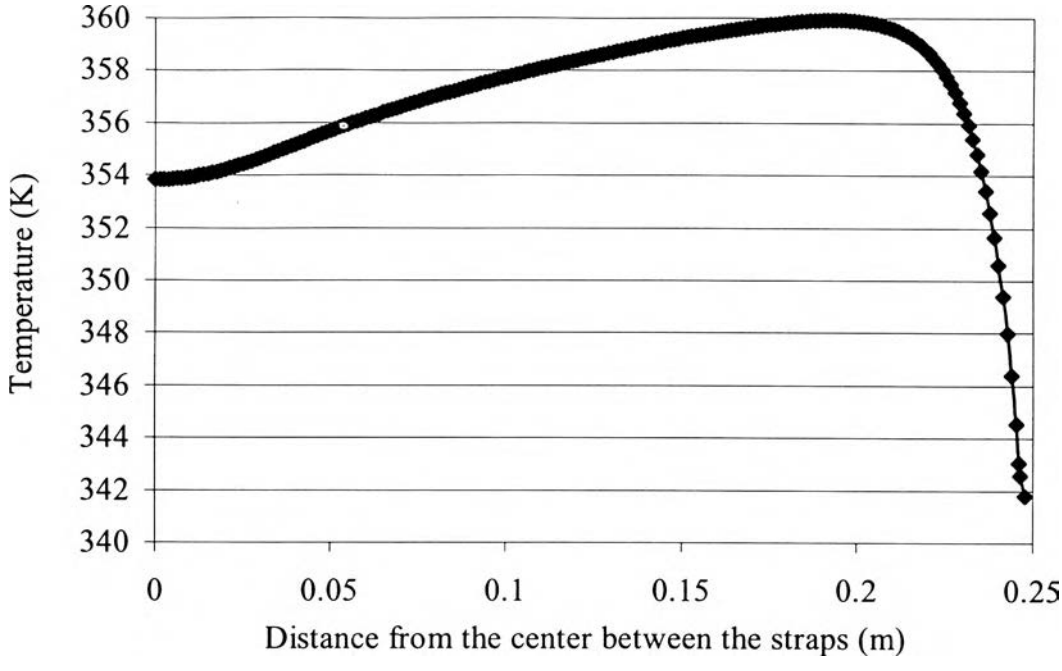

Figure 4.25 The temperature along the inside surface of the center tube, (R_1) for gamma heating at 10 W with using helium

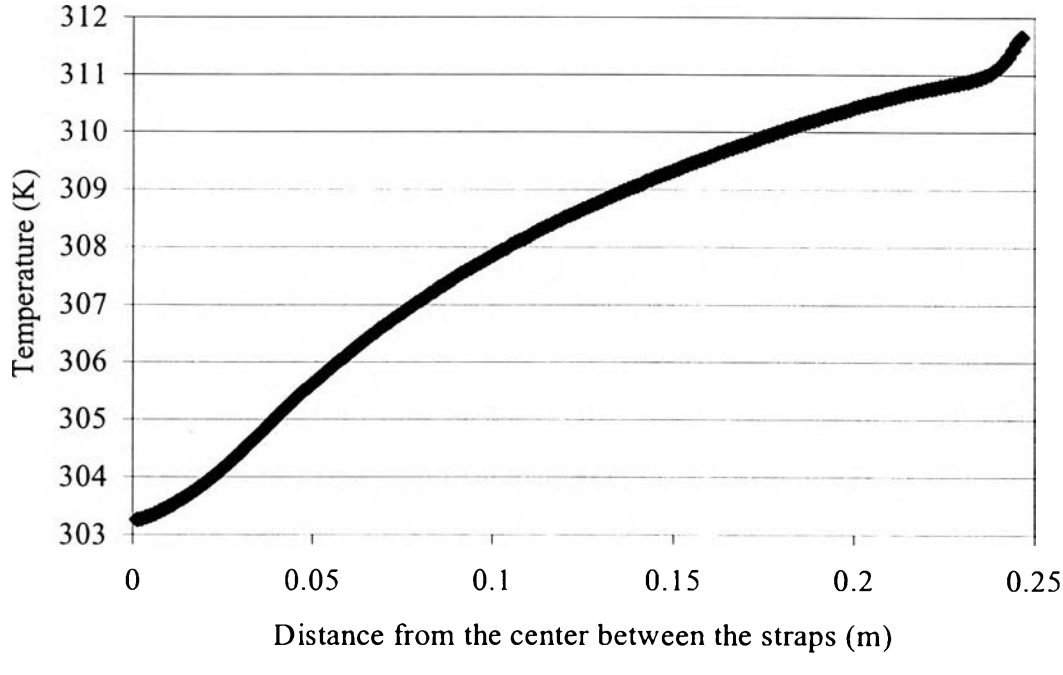

Figure 4.26 The temperature along the outside surface of the outer tube, (R_6) for gamma heating at 10 W with using helium

From Figures 4.19 to 4.26, the heat transfer characteristics are predicted in form of the temperature profiles. These graphs give nature of the heat flux patterns.

In the case of the temperature of the inside surface of the center tube, the temperature close to the right of the graphs, near the strap, is lower than the temperature close to the left, represented the center between 2 straps. On the other hand, the temperature of the outside surface of the outer tube close to the strap is higher than the value close to the center between 2 straps. This shows the heat flowing through the strap larger than flow through the fluid 2 next to the center tube to the upper layer because the thermal conductivity of the strap, which is zirconium, is larger than that of the fluid 2, air or helium. The values of thermal conductivity are 0.026, 0.152 and 22.7 W/m-K for air, helium and zirconium, respectively that were used as the initial conditions in FLUENT program. The largest amount of heat is passed through the strap or the area at the right hand side of the flux tube.

For the case of the inside surface of the center tube with air as the fluid 2 and the heating rate at 1.11 W/g, Figure 4.19, the electrical heating case, is compared to Figure 4.23, the gamma heating case. The hot spot of the gamma heating case is higher than of the electrical heating case. For the electrical heating case, there is only the bottom layer generating heat, while the gamma heating case had the heat generation in all solid phases and liquid 1. Thus more heat is generated for the case of gamma heating. Then, less heat is allowed to flow to the next layer.

In the same manner, the comparison between Figure 4.21 and Figure 4.25 for the consideration of the inside surface of the center tube with helium as the fluid 2 and the heating rate at 1.11 W/g also gives as similar result. The hot spot in the gamma heating case is higher than in the electrical heating case.

In the situation of using the electrical heating and the heating rate at 1.11 W/g, the comparison between Figure 4.19 and Figure 4.21 shows that the hot spot in air case is less pronounced than in helium case owing to the higher value of thermal conductivity of helium. The result from comparing Figure 4.21 and Figure 4.25 for the gamma heating case is also similar in that heat can be transferred through helium more readily than air and the hot spot for helium is more pronounced.

From Figure 4.19 to Figure 4.26, the strap strongly influences the temperature difference in both gamma heating and electrical heating. According to the maximum temperature, in the irradiative heating, this value is more than that of electrical heating under the same condition of the heat generation per unit volume.

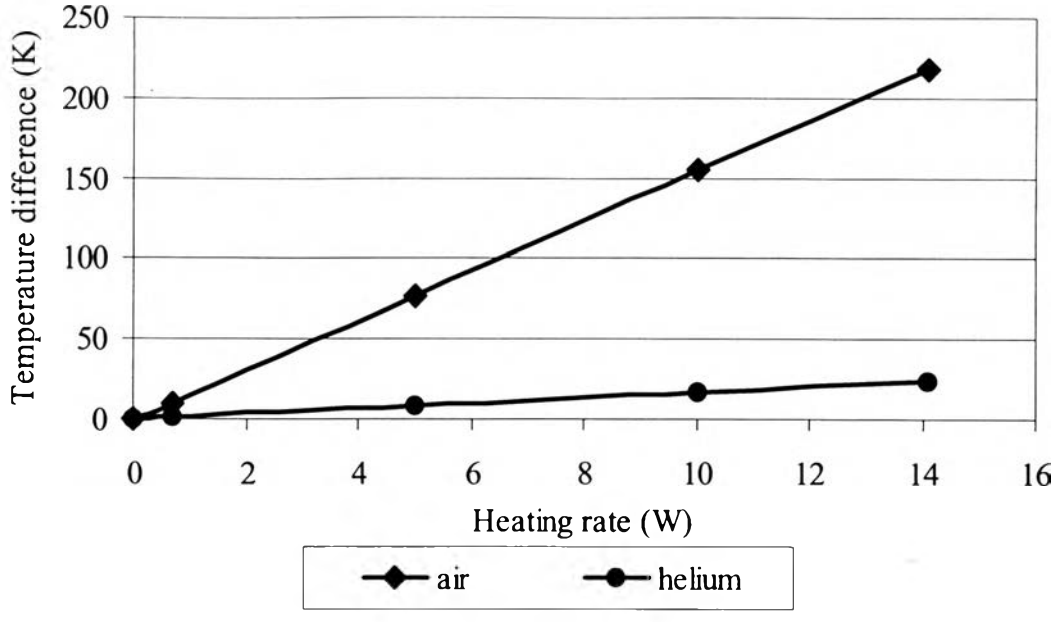

Figure 4.27 Temperature difference between the strap and the center between two straps vs. heating rate with using electrical heating

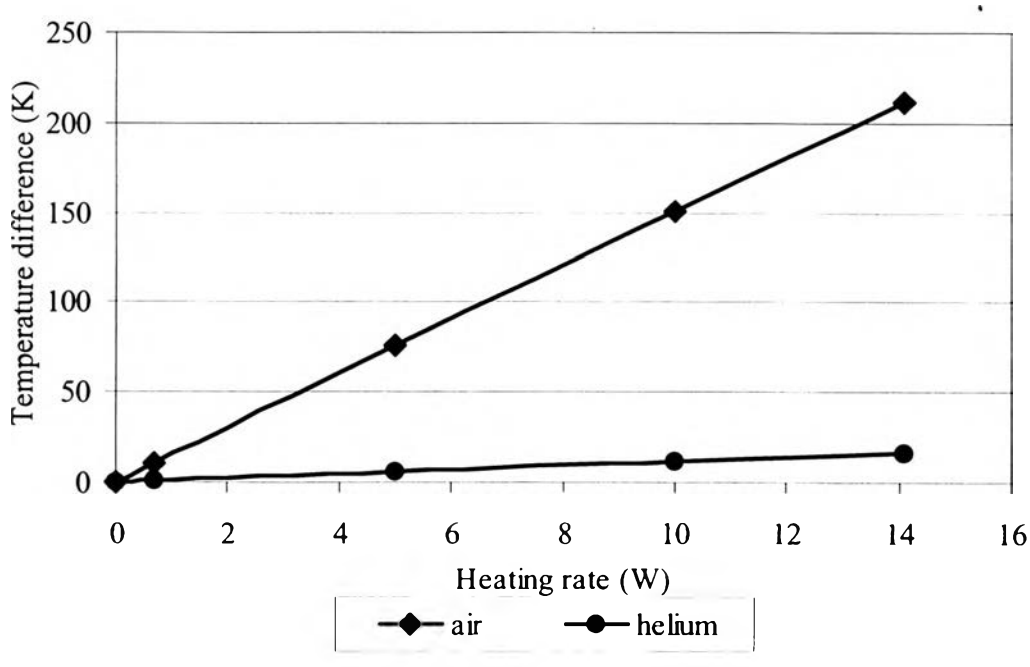

Figure 4.28 Temperature difference between the strap and the center between two straps vs. heating rate with using irradiative heating

Figures 4.27 and 4.28 are the relationship of the temperature difference between the strap and the center between the straps with the heating rate for the case of the electrical heating and the gamma heating, respectively. These pictures show that the temperature difference with using air and helium is increased with increasing the amount of the heating rate. Both figures give the same relationship as in the experimental result with using test cell as shown in Figure 4.9. The temperature difference with using air is higher than one with using helium. It is due to the different heat transfer characteristic between air and helium. Air and helium were used as the stagnant gas in the layer between the center cylinder represented the bundle of detector wells, and the inner tube represented the capsule tube. The slope of graphs shown in Figures 4.27 and 4.28 is the value of heat transfer coefficient. The heat transfer coefficient of air is about 9 time more than that of helium. For the higher heat transfer coefficient, it causes the less temperature difference. The temperature difference of air is more pronounce than that of helium. From these two graphs, temperature distribution can be reasonably to determine the amount of heating rate in the nuclear reactor by using the vertical flux detector assembly.